JOURNAL OF CHEMICAL INFORMATION AND MODELING

Article

pubs.acs.org/jcim

Structure−Activity Relationships and Identification of Optmized CC-Chemokine Receptor CCR1, 5, and 8 Metal-Ion Chelators

Alexander Chalikiopoulos,[†] Stefanie Thiele,[‡] Mikkel Malmgaard-Clausen,[‡] Patrik Rydberg,[†] Vignir Isberg,[†] Trond Ulven,[§] Thomas M. Frimurer,[⊥] Mette M. Rosenkilde,[‡] and David E. Gloriam*[,†]

[†]Department of Drug Design and Pharmacology, [‡]Department of Neuroscience and Pharmacology and [⊥]The Novo Nordisk Foundation Center for Basic Metabolic Research, Faculty of Health and Medical Sciences, University of Copenhagen, DK-1165 Copenhagen, Denmark

[§]Department of Physics, Chemistry and Pharmacy, University of Southern Denmark, Campusvej 55, DK-5230 Odense, Denmark

Supporting Information

ABSTRACT: Chemokine receptors are involved in trafficking of leukocytes and represent targets for autoimmune conditions, inflammatory diseases, viral infections, and cancer. We recently published CCR1, CCR8, and CCR5 agonists and positive modulators based on a three metal-ion chelator series: 2,2′-bipyridine, 1,10-phenanthroline, and 2,2′;6′,2″-terpyridine. Here, we have performed an in-depth structure−activity relationship study and tested eight new optimized analogs. Using density functional theory calculations we demonstrate that the chelator zinc affinities depend on how electron-donating and -withdrawing substituents modulate the partial charges of chelating nitrogens. The zinc affinity was found to constitute the major factor for receptor potency, although the activity of some chelators deviate suggesting favorable or unfavorable interactions. Hydrophobic and halogen substituents are generally better accommodated in the receptors than polar groups. The new analog brominated terpyridine (**29**) resulted in the highest chelator potencies observed so far CCR1 (EC_{50}: 0.49 μM) and CCR8 (EC_{50}: 0.28 μM). Furthermore, we identified the first selective CCR5 agonist chelator, meta dithiomethylated bipyridine (**23**). The structure−activity relationships contribute to small-molecule drug development, and the novel chelators constitute valuable tools for studies of structural mechanisms for chemokine receptor activation.

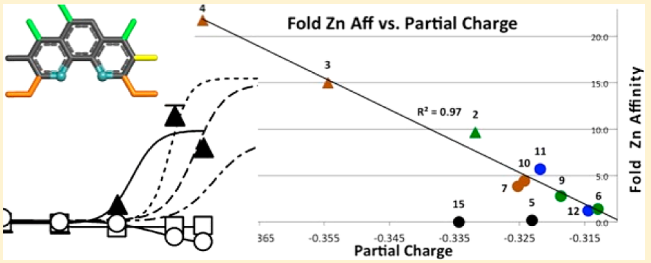

INTRODUCTION

Chemokine receptors belong to Class A G protein-coupled (GPCR)/7-transmembrane (7TM) receptors, the largest group of membrane proteins in the human genome,[1] and the group most extensively exploited by current drugs.[2] Together with their peptide ligands, chemokine receptors mediate leukocyte migration and play a crucial role in the immune system during homeostasis and inflammation. The chemokine system has been addressed as potential target in e.g. autoimmune diseases, allergy, inflammation, allograft rejection, angiogenesis, cancer development and progression, and HIV-infection.[3−5] Consisting of approximately 50 chemokine ligands and 18 receptors, the system is characterized by some redundancy and promiscuity. This is speculated to cause the lack of clinical efficacy observed for most drug candidates, and to solve this problem, the design of promiscuous chemokine receptor ligands has been suggested.[6,7]

Chemokines are 8−12 kDa peptides with 2−4 conserved cysteines which engage in disulfide bridges shaping chemokines into a flexible N-terminus before the first cysteine, followed by a core domain containing an N-loop, a 3_{10}-helix, a three-stranded β-sheet, and a C-terminal α-helix.[8] The pattern of the first two cysteines classifies the chemokines and their receptors into the two major CC- and CXC-groups. Two minor groups comprise the CX_3C- and XC-receptor and -ligands.[9] Binding of chemokines to a receptor is mediated by the ligand core domain and receptor extracellular domains, while the chemokine N-terminus can contribute to the signaling properties via interaction with the receptor transmembrane domain.[8] Since chemokines are relatively large peptides, small molecule drug-candidates binding to chemokine receptors are often allosteric.[5,10]

A variety of natural protein functions are dependent upon or influenced by metal-ions. Zinc-ions are part of the active site in metalloenzymes, stabilize transcription factors in finger-binding motifs[11] and modulate dopamine transporters,[12] nicotinic acetylcholine,[13] ionotropic glutamate, tachykinin NK3,[14] GPR39,[15] melanocortin MC1 and MC4 receptors.[16] Metal-ions can also complex with chelators, small nucleophilic molecules, and this combination has proven very useful for pharmacological and structure−function studies. Within the GPCR/7TM field, the introduction of metal ion sites in the $ß_2$-adrenergic,[17] CXCR3,[18] and NK_1[19] receptors laid the foundation of a receptor activation model, which proposed a concerted inward- and outward-movement of the extra- and

Received: July 3, 2013

   dx.doi.org/10.1021/ci4003848 | J. Chem. Inf. Model. XXXX, XXX, XXX−XXX

Chart 1. Chelator 1−20 Structures from Our Recent Publication[27] and the New Compounds, 22−29[a]

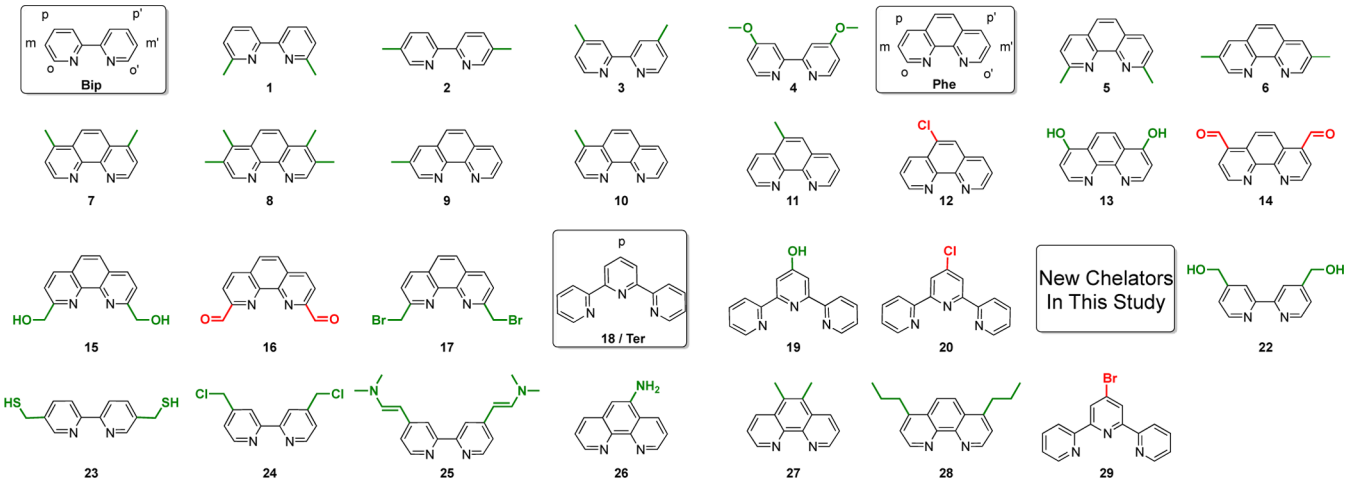

[a]Electron-donating and -withdrawing substituents are shown in green and red, respectively.

intracellular parts of TM-6, respectively.[20,21] This mode of activation has later been confirmed by active-state receptor crystal structures.[22−24]

Naturally occurring metal-ion chelator sites in chemokine receptors were first discovered in CCR1 and CCR5.[25,26] Our recent screening against all chemokine receptors uncovered additional targets, CCR4 and CCR8.[27] In other chemokine receptors, e.g. CXCR3 and ORF74-HHV8, metal-ion chelator sites have been successfully introduced.[18,28,29] Mutagenesis studies in CCR1, 4, 5, and 8 have identified a glutamate in TM-7 (position VII:06/7.39) as the metal-ion anchor.[10] This residue, which is centrally located in the binding pocket, is conserved in 13 of 18 chemokine receptors, but less than 1% of nonchemokine class A GPCRs/7TMs.[10] Importantly, for activation in CCR1, 4, 5, and 8, the metal-ion needs to be in complex with chelators and the chelator−receptor interactions serve to stabilize an active conformation. The chelator scaffolds, 2,2′-bipyridine (**Bip**), 1,10-phenanthroline (**Phe**), and 2,2′;6′,2″-terpyridine (**Ter**), can be substituted to alter size, shape, and physicochemical properties to probe the receptors for matching cavities. Moreover, electron-donating or -withdrawing substituent groups influence metal-ion affinity and aromatic chelator-receptor interactions by altering the partial charge of the chelating atoms and electron density in the ring systems.

The current study determines the structure−activity relationships for zinc affinity as well as CCR1, CCR8, and CCR5 potency and selectivity for our recently published set of 20 chelators.[27] These are applied prospectively to select a new series of optimized chelators.

RESULTS

Our recent analysis identified 20 chelators based on the **Bip**, **Phe**, and **Ter** scaffolds and a variety of substituents (Chart 1).[27] We observed that zinc affinities increase and decrease for electron-donating and -withdrawing groups, respectively (green and red in Chart 1). Receptor potencies seemed to display an overall increasing trend with the following respective substitutions: ortho, unsubstituted, meta, para, 5-position (**Phe**) relative to the chelating nitrogen atoms, although different groups in the same position can be unfavorable or favorable. This data indicates that the chelator activities can be modulated by increasing their zinc affinity, shape, and chemical properties. However, to generate viable optimization strategies, one needs to separate and quantify the effects that substituents have on zinc affinity and on receptor binding. In this analysis, we started by quantifying the effect that substituents have on the electron density of the chelating nitrogen atoms and found correlation to zinc affinities. We generated per-receptor structure−activity relationships (SAR) and strategies for optimization of both potency and selectivity. We present substitutions that lead to receptor inactivity due to steric hindrance or tautomerism. Finally, the SAR is validated and the information expanded by design and pharmacological testing of a series of eight new chelators.

Zinc Affinity Correlates to the Partial Charges of Chelating Nitrogen Atoms. Submicromolar zinc affinities (>6 log units) are displayed by the published **Phe** and **Ter**, but not **Bip**, analogs (Supporting Information Table SI1). Chelator analogs with electron-withdrawing groups generally display lower zinc affinities than compounds with electron-donating groups in the same positions (ortho: **16** vs **5**, para: **14** vs **7**, 5-pos: **12** vs **11**, **Ter** central para: **20** vs **19**). From this observation, we hypothesize that the substituents modulate zinc-binding strength by altering the partial charges of the chelating nitrogen atoms and that, if analyzed quantitatively, this information can be used to guide chelator optimization (choice of scaffold, position, and substitution group).

We performed density functional theory calculations to calculate partial charges of the chelating nitrogen atoms (Supporting Information Table SI1). Figure 1 shows that there is a strong correlation (R^2 = 0.97) between partial charges and fold affinity increase for the overall chelator set (excluding inactive and ortho-substituted compounds). The **Bip** (triangles) and **Phe** (circles) subsets display a similar trend supporting the shared overall relationship. The **Bip** analogs display higher negative partial charges and affinity increases than the **Phe** scaffold. This difference is clearest when inspecting the identical substitutions, i.e. meta (**2** vs **6**) or para (**3** vs **7**) di-Me. This can be explained by the fact that **Phe** distributes the added electron density also over a third ring.

Also the meta- (green), para- (brown), and 5-substituted (blue) subsets display the same correlations, higher measured zinc affinity for higher calculated partial charges, although the

dx.doi.org/10.1021/ci4003848 | J. Chem. Inf. Model. XXXX, XXX, XXX−XXX

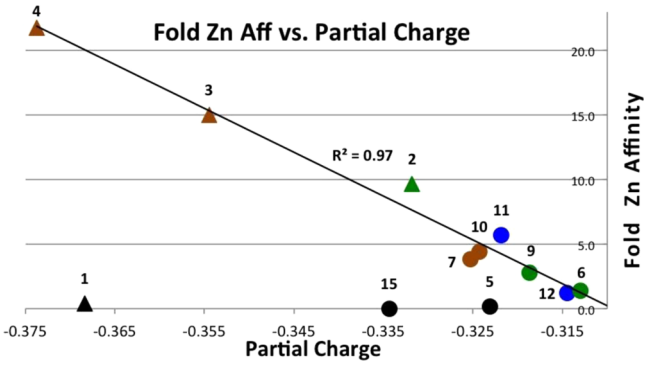

Figure 1. Correlation of the partial charges of chelating nitrogen atoms to fold zinc affinities (substituted analog over reference scaffold). The graph includes all Bip (triangles) and Phe (circles) analogs except the chelators lacking zinc activity (see methods). The effect of substitution is larger on Bip chelators, but the trend (slope) is similar to that of the Phe analogs. The meta (green), para (brown), and 5-position (blue) classes display similar relationships between partial charge and zinc affinity; whereas, the ortho-substituted (black) analogs all have close to no affinity (Supporting Information Table SI1). The zinc IC_{50} values were determined in competition assays using 1 μM FluoZin-3 as the reference ligand. The partial charges were calculated in Turbomole.[30]

extent of this effect varies somewhat. It is clear that the low zinc affinities of ortho-substituted (black) chelators are not due to weak partial charges. Instead, **Phe** ortho-analog Zn-affinities decrease as substituent sizes increase i.e. Br, Me, CHO, and CH═O for **17**, **5**, **15**, and **16**, respectively (Supporting Information Figure SI2). This suggests that the low Zn affinity of ortho-substituted chelators is due to steric hindrance between several chelators coordinating to the same metal-ion or between a chelator and the labeled competitor (FluoZin-3) used in the Zn affinity assays.

Receptor-Focused SAR of Published Metal-Ion Chelators. The following sections and figures serve to provide in-depth SAR for each receptor and to separate the effects that substituents have via zinc-binding and direct receptor interactions, something which is crucial in the rational design of optimized compounds. Figure 2 presents a per-receptor overlay of chelator zinc affinities and receptor potencies. Chart 2 provides a structural summary illustrating the fold effect (substituted analog relative to unsubstituted scaffold) of **Bip**, **Phe**, and **Ter** substituents on zinc affinity and receptor potencies.

The CCR1 potencies of the **Bip** and **Phe** series display a similar trend as the zinc affinities for the unsubstituted, 5-position, meta and para analogs (Figure 2a). In contrast, the

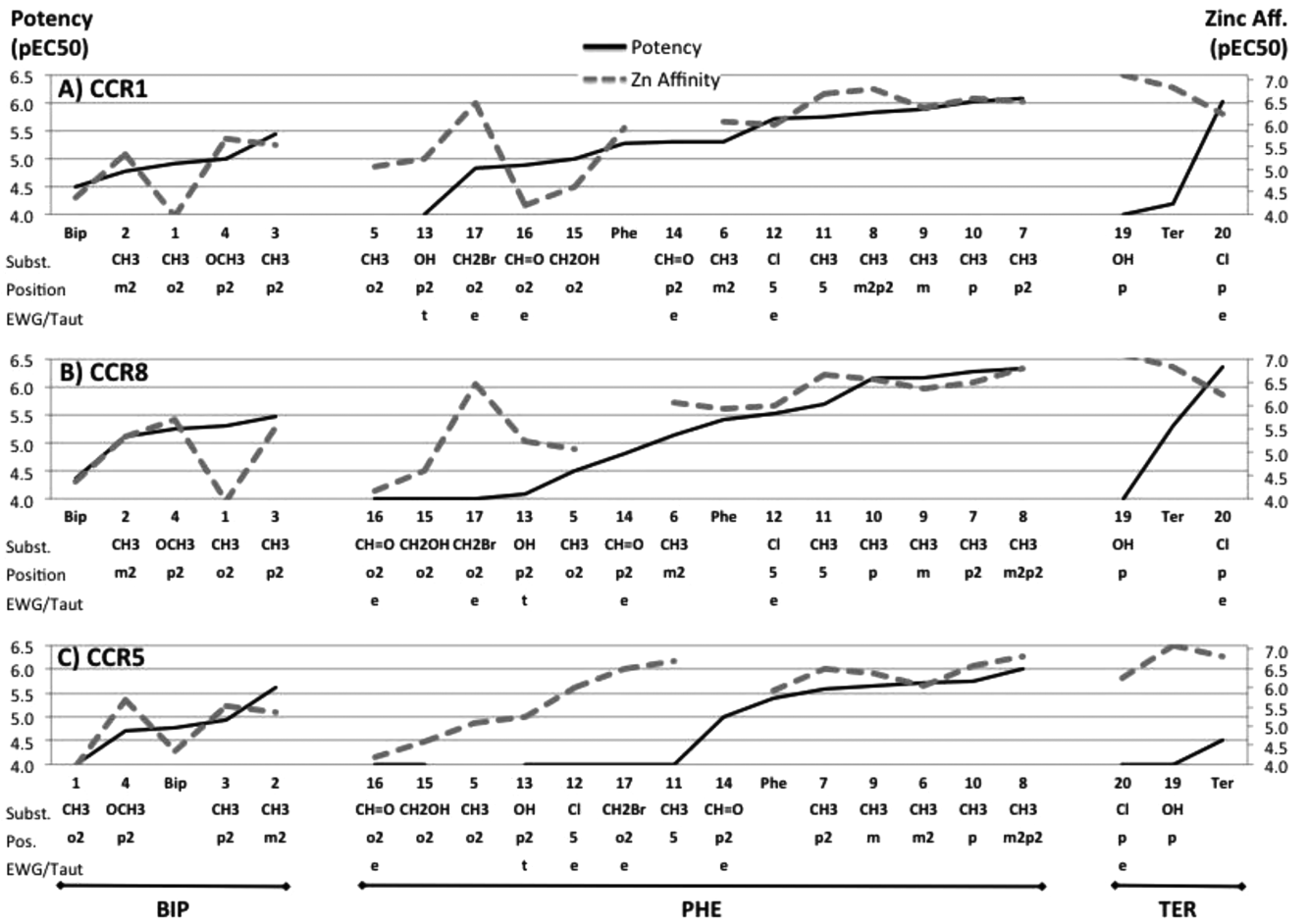

Figure 2. Comparisons of zinc affinities (dashed lines) and potencies in (A) CCR1, (B) CCR8, and (C) CCR5 (vertically) for the **Bip**-, **Phe**-, and **Ter**-series (horizontally). For the **Bip** and **Phe** series, the receptor potencies increase together with the zinc affinities in a general trend for (o)rtho, (m)eta, (p)ara, and (5)-substituted analogs. Chelators with (e)lectron-withdrawing or (t)automeric groups display lower affinities and/or potencies. The large varations in Zn affinity and receptor potency seen for some chelators derive from favorable or unfavorable interactions with the Zn binding assay competitor or receptor binding pockets, and this is described in the text.

dx.doi.org/10.1021/ci4003848 | J. Chem. Inf. Model. XXXX, XXX, XXX–XXX

Chart 2. Structural Depiction of Substitution (Fold) Effects on Zinc Affinity and Receptor Potencies[a]

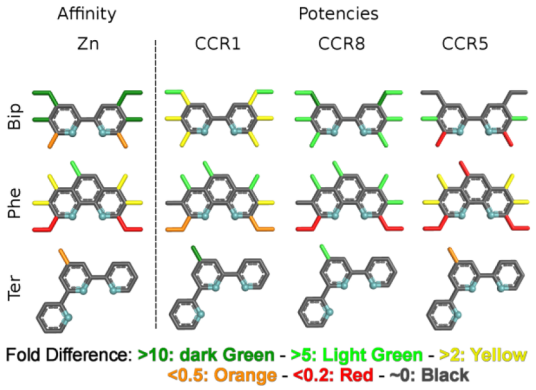

[a]The scaffolds are depicted in gray and chelating nitrogens in cyan spheres. Substituent colors indicate the fold activity difference upon substitution of the core scaffold. This scheme is simplified and does distinguish between electron-donating and -withdrawing groups, thus a few compounds could not be represented, specifically, the **Phe** analogs 17 (3.6 fold effect on zinc affinity), 5 (0.06 fold effect on CCR1 potency), and 19 (highest zinc affinity, but inactive at the receptors). For the **Ter** para-substitution, the chlorinated compound, 20, has been illustrated.

Ter chelators display opposite CCR1 potency and zinc affinity orders. Steric hindrance is displayed by ortho-substitution[27] and, to a lower degree, by meta-substitution of **Phe**; dimethylation (**6**) more so than monomethylation (**9**) (Supporting Information Table SI1). The highest CCR1 potencies are seen for the para di- (**7**, 1 μM) and monomethylated (**10**, 0.9 μM) **Phe** analogs. Furthermore, 1–2 μM potencies are seen for 5- (**11**), meta- (**9**), or meta- and para-methylated (**8**) **Phe** chelators and the para-chlorinated **Ter** (**20**). Notably, the three polar ortho-substituted analogs **1**, **16**, and **15** display a smaller penalty on potency in CCR1 than in CCR8 and CCR5 (Figure 2) giving rise to a 10, 7.7, and 6.7-fold selectivity, respectively (Supporting Information Figure SI1).

The unique accommodation in CCR1 suggests a lower steric hindrance effect. Moreover, molecular dynamics simulations of chelator–CCR1 receptor complexes with **15** showed extensive hydrogen-bond networks (unpublished data). The chelator hydroxymethyl groups form transient bonds to the residues glutamine Q284$^{7.36}$, tryptophan W90$^{2.60}$ via one water molecule. Furthermore, both the chelator and zinc ion partake in larger water-bonding networks that also include the tyrosines Y41$^{1.39}$, Y113$^{3.32}$, Y114$^{3.33}$, and Y225$^{6.51}$. Furthermore, the zinc atom anchor, glutamic acid E287$^{7.39}$, participates in this network and can also hydrogen bond directly to Y225$^{6.51}$. The simulations indicate that the pocket is well solvated and that hydrogen bonds, direct and water-mediated, play a role in the binding of the metal-ion–chelator complex. This has previously been shown for other GPCR ligands and the computational studies of water-bonding networks have greatly evolved, a leading example being the recent analysis of adenosine A2A antagonists.[31] These observations are in line with both potency and selectivity values that increase in the same order as hydrogen-bonding strength, i.e. bromomethyl (**17**), formyl (**16**), and hydroxymethyl (**15**) (Supporting Information Table SI1). However, these chelators are suboptimal due to the relatively low potencies (10–15 μM) and ability to induce a receptor response; efficacies are 46, 26, and 44% for **15**, **16**, and **17**, respectively.

As previously described,[27] CCR8 displays a similar potency trend as CCR1 for the **Bip**, **Phe**, and **Ter** series (Figure 2b). However CCR8 does not share the general acceptance of ortho-substitutions observed for CCR1, although ortho di-Me substitution (**1**) increases potency of **Bip**. The **Bip**, but not **Phe**, scaffold is able to rotate the pyridine rings giving the possibility to direct the ortho-substituents away from steric clashes with the receptor. Five chelators display submicromolar (0.4–0.7 μM) CCR8 potencies: **Phe** with meta (**9**), para (**7**

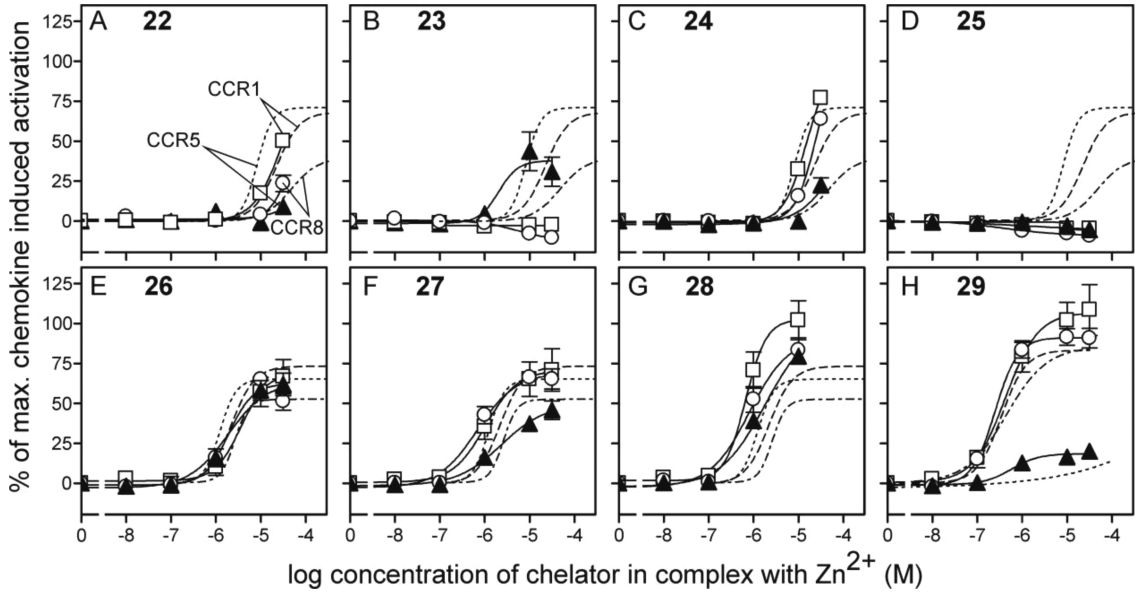

Figure 3. Activity of a new set of metal ion chelators on CCR1, CCR8, and CCR5. The compounds were tested for their ability to induce IP_3-accumulation in COS-7 cells transiently transfected with CCR1 (□), CCR8 (○), or CCR5 (▲) and the promiscuous G protein G_{qi4myr}. The curves are normalized to maximal chemokine-induced activation of each receptor (CCR1:CCL3, CCR5:CCL5, and CCR8:CCL1). Dashed lines represent controls, i.e. **Bip** activity for compounds 22–25, **Phe** for 26–28, and Zn-**Ter** for 29.

dx.doi.org/10.1021/ci4003848 | J. Chem. Inf. Model. XXXX, XXX, XXX–XXX

Table 1. New Chelator Zinc Affinities (IC_{50}, μM), Potencies (EC_{50}, μM), and Efficacies (%)[a]

		Zn(II) affinity					CCR1							CCR8								
	Cmpd	pIC50	SEM	IC50	Fold	(n)	pEC50	SEM	EC50	Fold	Efficacy	SEM	(n)	pEC50	SEM	EC50	Fold	Efficacy	SEM	(n)	pEC50	SEM
	Bip	4.4	0.05	43.6	1.0	4	4.5	0.05	32.6	1.0	79.6	4.2	37	4.4	0.03	42.0	1.0	70.4	7.9	41	4.8	0.05
	Phe	5.9	0.07	1.2	1.0	4	5.3	0.06	5.4	1.0	84.3	3.7	33	5.4	0.04	3.8	1.0	67.9	8.8	40	5.4	0.08
Bip	**22**	4.8	0.02	17.3	2.5	3	4.7	0.05	20.0	1.6	NA	-	3	4.2	0.11	63.1	0.7	NA	-	3	4.0	0.00
	23	5.8	0.01	1.5	28.5	3	-	-	-	-	-2.3	0.4	3	-	-	-	-	-14.2	3.7	3	5.9	0.03
	24	5.1	0.03	7.8	5.6	3	4.9	0.08	12.6	2.6	NA	-	3	4.8	0.07	15.8	2.7	NA	-	3	4.1	0.12
	25	5.6	0.02	2.4	18.3	3	-	-	-	-	-2.6	1.6	3	-	-	-	-	-4.7	4.0	3	-	-
Phe	**26**	6.3	0.02	0.5	2.3	3	5.4	0.06	3.7	1.5	72.2	14.2	3	5.9	0.06	1.3	3.0	60.4	4.4	3	5.7	0.03
	27	6.8	0.04	0.2	7.7	3	6.0	0.02	1.1	4.9	76.5	17.2	3	6.1	0.07	0.8	5.0	66.9	2.9	3	5.7	0.13
	28	6.8	0.04	0.2	7.4	3	6.2	0.07	0.7	7.9	110.6	15.7	3	6.1	0.23	0.9	4.4	92.8	14.5	3	5.9	0.08
Ter	**29**	6.1	0.05	0.8	0.2	3	6.3	0.10	0.5	127.6	112.6	19.8	4	6.6	0.07	0.3	17.9	91.4	5.9	4	6.2	0.09

[a]The zinc IC_{50} values were determined in competition assays using 1 μM FluoZin-3 as the reference ligand. The receptor potencies (EC_{50}) were determined using IP_3[27] and scintillation proximity assays. Efficacies were calculated with 0 set to the average bottom values and 100 to the top of the endogenous ligands; CCR1:CCL3, CCR5:CCL5, and CCR8:CCL1. Due to the low efficacies no potencies are reported for **23** and **25** (except **23** in CCR5). NA (not available): The given E_{max} measurements did not reach a plateau. The color-scale of the EC_{50} and fold affinities and potency values ranges from green (best) to red (worst).

and **10**), and meta and para (**8**) methyl-substituents and para-chlorinated **Ter** (**20**). The highest selectivity, 6,4-fold, is displayed by **Ter**; whereas, no other compound reaches above 2.5 fold (Supporting Information Figure SI3).

CCR5 is only activated by unsubstituted and meta- or para-substituted chelators (Figure 2). Whereas CCR1 and CCR8 can accommodate **Bip** ortho- (**1**) and **Phe** 5-substitutions (**11** and **12**), these result in inactivity in CCR5 indicating that it has no room on these two opposite sides of the chelators. Also para-substitution is less favorable in CCR5 and potency is higher for para mono- (**10**) than dimethylated (**7**) **Phe**, as opposed to the other two receptors. Furthermore, the potency of **4** (para di-OMe **Bip**) is slightly decreased (0.9 of **Bip**) in CCR5, while it is increased (3.2 and 7.7 fold, respectively) in CCR1 and CCR8 (Supporting Information Table SI1). In the **Ter** series, the unsubstituted **Ter** displays low (32 μM) CCR5 activity; whereas, both para-substituted analogs, including **20** with 0.4−0.9 μM potency in the other receptors, are inactive. The highest CCR5 potencies are shown by three **Phe** analogs: **8** (1 μM; meta and para di-Me **Phe**), **10** (1.8; para Me), and **6** (1.9; Meta di-Me). Selectivity is seen for meta dimethylation but is only 3.2- and 2.6-fold for the **Bip** (**2**) and **Phe** (**6**) analogs, respectively (Supporting Information Figure SI3).

Validation of SAR and Identification of New Optimized Chelators. Based on the SAR presented above, and with a strategy to include untested shapes and functionalities, we tested a new series consisting of 5 **Bip** (**22**−**25**), 3 **Phe** (**26**−**28**), and 1 **Ter** (**29**) chelator analogs substituted with polar, halogen, and alkyl substituents (Chart 1). Figure 3 presents the dose−response curves of these compounds on CCR1, 5, and 8. Table 1 contains the EC_{50} values for zinc affinities and receptor potencies, efficacies as percentage of the response compared to an endogenous ligand and selectivities. Finally, Figure 4 plots an overview of the potency, efficacy, and selectivity of the best chelators for each receptor.

CCR1 Chelators. The new chelator series resulted in four new molecules with submicromolar activity and structural diversity covering all three scaffolds and substitutions with thiomethyl (**23**), primary amine alkene chain (**25**), propyl (**28**), and bromine (**29**) (Figure 4A). **23** and **25** display the best potencies (0.20 and 0.32 μM, respectively) and relatively good selectivity (6.3 and 3.8 fold, respectively), but their efficacies are so low (2.3 and 2.6%, respectively) that they have been disregarded. The other two new chelators **28** and **29** have good potencies (0.5 and 0.7 μM, respectively) and efficacies (113 and

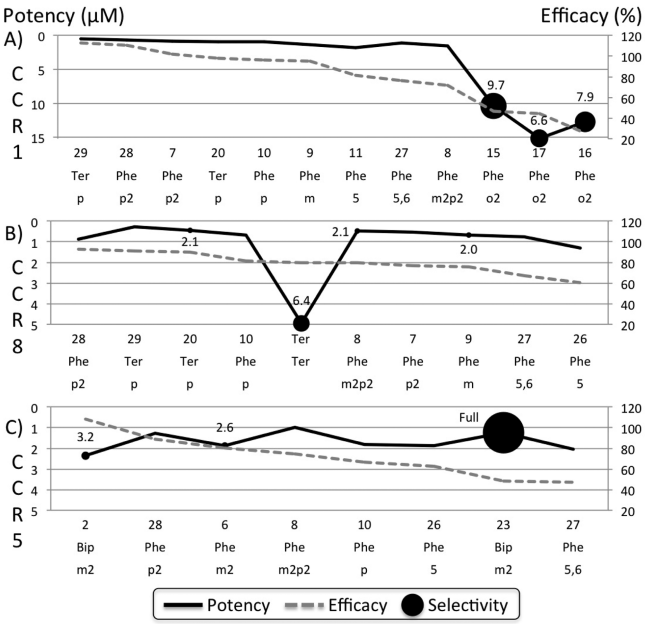

Figure 4. Potency, efficacy, and selectivity of the best lead chelators for (A) CCR1, (B) CCR8, and (C) CCR5 (efficacy >20% and potency <2 μM or selectivity >2-fold). Selective chelators are displayed as circular markers in the potency graphs and are defined both by with numbers and relative size. The selectivity is defined as the highest over the second highest potencies (EC_{50} values) for a compound in any receptors (see Supporting Information Figure SI3). The selectivity of **23**, which only stimulates CCR5, was set to 15 in the graph.

111%, respectively) but are not selective. In terms of selectivity, the *ortho para*-hydroxymethylated **Phe**, **15**, is most promising (10-fold selectivity), but both its potency (9.7 μM) and efficacy (46%) are suboptimal. For these reasons and the relatively broad existing set of ortho-substituted analogs, no new ones were tested here. Future strategies to achieve improved analogs could be based on the combination of observed substitutions to generate both high potency and selectivity. For CCR1, one plausible approach could be to design a **Phe** analog containing both the hydroxymethyl of the selective **15** and potency-increasing substituents in the para- and 5-positions (Chart 2).

CCR8 Chelators. The new chelator series added four more chelators, **26**−**29**, with 2 μM or better CCR8 potency, the most potent (0.28 μM) being the centrally para-brominated **Ter**, **29**

dx.doi.org/10.1021/ci4003848 | J. Chem. Inf. Model. XXXX, XXX, XXX−XXX

(Figure 4B). Unfortunately, the selectivity is still limited to the 6.4-fold CCR8 preference displayed by **Ter**. The centrally para-chlorinated (**20**) and -brominated (**29**) **Ter** analogs display lower selectivity, 1.8- and 2.1-fold, respectively. Thus, further optimization of CCR8 activity could focus on nonhalogens in this position or substitution at other sites, such as the western and eastern rings, which have not yet been derivatized. Moreover, Chart 2 shows that CCR8 potency increases by substitution at **Bip** in the ortho, meta, and para positions as well as **Phe** in the meta, para, and 5-positions. Therefore, an alternative route could be to test combinations of several of these substitutions to see if potency increases more for CCR8 than CCR1 and CCR5.

CCR5 Chelators. Five new chelators [**23**, **26**−**29**] have a CCR5 potency of 2 μM or better (Figure 4C). Surprisingly, the 5-substituted chelators **26** and **27** are included in this list, directly in contrast to the inactivity previously observed for **11** and **12**. The most potent (0.66 μM) chelator is the centrally para-brominated **Ter** analog **29** (Table 1), which however displays a (1.8 fold) preference for CCR8 and has very low (19%) efficacy in CCR5. With regard to selectivity, the original series demonstrated that meta dimethylation of both **Bip** (**2**) and **Phe** (**6**) generates a CCR5-preference; 3.2- and 2.6-fold, respectively. To investigate if a longer meta-substituent could further increase CCR5 selectivity, we acquired and tested the meta dithiomethylated **Bip** (**23**). **23** succeeded in achieving fully selective agonism at CCR5, while being inactive or very weak inverse agonists in CCR1 and CCR8. Also its potency, 1.3 μM, is among the highest observed for CCR5, while the efficacy is at medium level (46%). To induce a higher receptor response, it would be warranted to complement **23** with potency-increasing para-substituents (Chart 2) or investigate the effect of exchange of the thiols for other groups; both hydrophobic and polar. However, even with the current efficacy **23** could be considered suitable for many applications as a pharmacological tool compound.

Additional Physicochemical Properties of Substituents Affect Chelator Activities. *Halogen Substituents May Be Favored by the Receptors, While Polar Are Not.* Methylation of **Bip** and **Phe**, in the correct positions as described above, increases receptor potencies also beyond what can be expected from just the electron-donating effect. This suggests that lipophilicity of substituents is a main factor for receptor potencies, at least close to the aromatic pyridine rings. The old and new chelator series also include a number of halogen and polar substituents. These explore the effect of lipophilicity but also introduce the possibility of halogen- and hydrogen-bonding, respectively. A mechanism-of-action study with mutagenesis and ligand docking is ongoing and will be published later; below, the purely ligand-based observations are described.

Halogens are weakly electron-withdrawing and consequently reduce the partial charges of chelating nitrogens, thus lowering zinc affinities. However, 5-chlorination of **Phe** (**12**) leads to 2.8-fold increased potency in CCR1 (Supporting Information Table SI1). This effect could be solely due to lipophilic interaction as the 5-methylated **Phe** (**11**) has a 3.1-fold increase potency. Furthermore, para-chlorination of **Ter** (**20**), although giving reduced zinc affinity, substantially increases the CCR1 and CCR8 potencies (0.3-, 69-, and 11-fold, respectively). The para-brominated **29** has even higher potencies and can even activate CCR5. In contrast, a polar hydrogen-bonding substituent, OH, in **19** results in inactivity. **24**, para dichloromethylated **Bip**, was hypothesized to have a high potency, as the methyl spacers between the pyridines and chlorines avoid the electron-withdrawing effect (as would have been seen in 4,4′-dichloroBip). However, although the Zinc affinity and CCR1 and CCR8 potencies were elevated (5.6, 2.6, and 2.7 fold of **Bip**s, respectively), they were more so by para dimethylation (**3**) (15, 9.0, and 13-fold of **Bip**s, respectively). Two other new chelators (**25** and **28**) are para-substituted with longer chains and yet display higher potencies indicating that there is not a large steric hindrance effect. Taken together, the current data shows that halogenation is favorable in the 5-position of **Phe** (CCR1) and para-position of **Ter**, but probably not the para-position of **Phe**.

All three scaffold series comprise analogs that suggest that polar substituents are not well-accommodated by the receptors. The **Bip** para dimethoxylated chelator (**4**) had the highest zinc affinity among the published compounds, while its receptor potencies were lower than for the methylated analog (**3**) (Supporting Information Table SI1). This effect is even clearer for the new chelator **22**, that has para dihydroxymethyl substituents, in which the electron-donating effects of the oxygen atoms are removed by the methyl spacers. Its potencies are down to 20, 63, and >100 μM in CCR1, CCR8, and CCR5, respectively. Also the zinc affinity is low, 17 μM, indicating unfavorable interactions between multiple chelators on the same zinc ion or to the labeled competitor. The high potency of **25** could be seen as contradictory as it is even larger than **22**, but the tertiary amine is less polar than the hydroxyl functionality and the ethylene linkers could provide both electron density to the pyridine rings and form favorable hydrophobic interactions with receptor residues. On the **Phe** scaffold, the **14** para diformyl substitution (moderately electron withdrawing) led to decreased (CCR8: 0.2-fold and CCR5: 0.4-fold) or unaffected (CCR1: 1.1-fold) potencies. The 5-aminated **Phe**, **26**, displays increased receptor potencies; however, the effect is smaller than expected considering that the primary amine is one of the strongest electron-donating groups. Finally, **Ter** displays the strongest example as the para OH-substitution (strongly electron donating) in **19** nearly doubles the zinc affinity but abrogates receptor potencies.

Tautomer and Metal-Binding States of 13 Explain the Low Zinc Affinity and Lack of or Low Receptor Potencies. Even at physiological pH, a small molecule can adopt multiple alternative tautomer or ionization states this can result in protonation of the chelating atoms. We analyzed chelator states using Epik applying the OPLS-2005 force field.[32] The pH was set to 7.2 ± 0.2, and the calculation was set to include metal binding states. We found that for **13** (para dioxygenated **Bip**), the two states with the lowest tautomer/ionization penalties, which represent the most frequent forms, are protonated on both or one of the chelating nitrogen atoms (Supporting Information Chart SI4). This explains it is relatively (for a para-substituted chelator) low zinc affinity (5.9 μM), very poor potency in CCR8 (79 μM), and inactivity at CCR1 and CCR5. A further explanation to the low/absent potencies is that chelation at the negatively charged oxygen atom in **13.2**, which is presented by Epik as a metal-binding-specific state, could result in a complex with a geometry that does not fit inside the receptor binding pockets.

DISCUSSION

This study has analyzed the correlations between substituents on both zinc affinity and receptor interactions. Increasing the

dx.doi.org/10.1021/ci4003848 | J. Chem. Inf. Model. XXXX, XXX, XXX−XXX

zinc affinity can be a strategy to achieve higher receptor potencies. However, the data for the four **Ter** compounds raises two rather puzzling questions: (1) Why does adding an electron-withdrawing para halogen (**20** and **29**) to **Ter** increase potencies in CCR1 and CCR8 (**20** 69- and 11-fold and **29** 128- and 18-fold, respectively) and (2) why does **19** (central para O) have the highest zinc affinity of all chelators (0.08 μM) and yet fails to activate the receptors? As presented here, halogens seem to be better accommodated than polar groups, but this is not enough to explain these phenomena. In line with our previous discussion,[27] a more compelling answer could be that **19** and to some extent **Ter** have so high zinc affinity (0.08 and 0.15 μM, respectively) that it outcompetes the binding of the receptor to the metal-ion by obtaining full 6-coordination by two terpyridine chelators. The electron-withdrawing halogen in **20** (0.59 μM) could avoid this effect. This would suggest that chelator potencies can only be optimized to a certain point by increasing the zinc affinity (threshold in the range between 0.15 and 0.59 μM).

The analyzed **Bip** series displays stronger partial charges at chelating nitrogens than the **Phe** (−0.37 to −0.33 vs −0.33 to −0.28). However, Phe chelators display higher zinc affinities (**Bip** 1.5−44 μM and **Phe** 0.21−5.9 μM, excluding the ortho-substituted) and receptor potencies, with the exception of **23** activation of CCR5 (Supporting Information Table SI1). The **Phe** increase in receptor potencies could partly be explained by interactions with the additional aromatic ring, but this effect is too small to be the only factor and it does not explain the elevated zinc affinities. A more plausible explanation is the advantage of **Phe** having the chelating nitrogen atoms locked to the same side, whereas in **Bip** the pyridine rings must first be rotated. The (energy and affinity) cost of this rotation could be attributed to entropic loss or that **Bip** largely adapt a confirmation with the N-lone pairs in opposite directions to cancel internal dipolar moments. We performed density functional theory calculations with the **Bip** bond dihedral set to 0 and 180°, respectively, and found that energy cost to twist one pyridyl back is 18.7 kJ/mol. This probably makes internal dipolar moments the largest contributor to the observed affinity difference, whereas the entropic loss is quite small.

The **Ter** scaffold is different in that it has three chelating atoms making the chelation stronger, despite the energy cost of pyridyl-rotation as described above for **Bip**. Accordingly, the chelator with the highest zinc affinity, **19**, is a **Ter** analog as is also the most potent CCR1 and CCR8 compound **29** (highest potency also in CCR5, but only 19% efficacy). However, there are many **Phe** chelators with similar zinc affinities and potencies. The advantages of the **Phe** scaffold are that it displays higher ligand efficiency (activity/size) and offers more substitution sites. Arguably, this makes the **Phe** scaffold the most suitable for further optimization, but the **Ter** scaffold is pharmacologically interesting because it can display both positive allosteric and agonistic modes of activity.[27]

With regard to receptor potencies this analysis succeeds our recent chelator identification report[27] by describing per-receptor SAR forming optimization strategies that have been tested with new compounds. This study identified higher potency compounds for all targets, importantly also after taking into account that some high potency compounds have low efficacies. Notably, a number of chelators could achieve receptor efficacies higher than the endogenous ligands (CCR1 **4**, **7**, **28**, and **29**; CCR8 **4**; and CCR5 **2**). For some chelators the efficacy is limiting; all chelators with more than 4-fold selectivity display less than 50% efficacy (except the 80% Ter efficacy in CCR8). Efficacy, is difficult to understand, as even very similar compounds may have opposite intrinsic activities, and thereby span from antagonists to full agonists. Among chemokine receptors, this has been observed in CXCR3, where a series of biaryl-based antagonists were changed to full agonists by the moving of a halogen atom from the meta- to the ortho-position, and where even subtle changes in the biaryl dihedral angle resulted in dramatic efficacy change.[33] Similar efficacy changes were observed in the ghrelin receptor, where the depths of ligand anchorage determined efficacy.[34] Another approach has been to understand efficacy from the ligand binding kinetics. Thus recent studies in the muscarinic M3 and the adenosine A2 receptors have shown that the receptor residence time of a given agonist is positively correlated with the efficacy, whereas this is not the case for agonist affinity.[35,36] According to this, efficacy is simply determined by the time a given agonist is bound to the receptor, yet the minor structural changes in the agonists mentioned above, could also course these changes, and thereby combining the structural and the kinetic aspect of understanding efficacy.

We also identified the first selective CCR5 chelator agonist, **23**. Selective ligands can be a prerequisite for some pharmacological studies, whereas in others a broader target profile may actually be advantageous. Specifically, multireceptor targeting has been suggested as solution to overcome the promiscuity of the chemokine system by blocking compensatory mechanisms.[6,7] A number of chelators (e.g., **11**, **12**, **14**, and **20**) display dual CCR1-CCR8 activity, with no or weak CCR5 potency. Such activity has been reported previously for the small molecule agonist LMD-559.[37,38] No other receptor pairs in our series have more than 3.2-fold selectivity. However, triple activity with at least 2 μM potency is seen for six chelators (**7**, **8**, 9, **10**, **28**, and **29**). Dual-steric ligands have also been reported previously for CCR2-CCR5 (TAK-779 and TAK-652[35,36]), CCR1-CCR3 (UCB35625[37]), CXCR1-CXCR2 (reparixin[38] and SCH-527123[39]), CXCR4-CCR5,[40] and CCR2-CXCR2 (thiazolo(4,5-*d*) pyrimidines[41]).

The metal-ion and chelator combination constitutes a double component system, which is more complex than ordinary small molecules. However, the utility of the concept of interchangeable chelating small molecules is not direct identification of structures to serve as lead drugs. Instead, it is a means to effectively probe and compare receptor binding sites to determine which sizes, shapes, and chemical functionalities can be accommodated. The structure−activity relationships that are obtained can subsequently form the basis for a translation into small molecule bioisosteres that share the concept of an aromatic system next to a positive charge. The metal-ion chelators may also be applied as tool compounds with different pharmacological effects. Our previous study demonstrated agonism, ago-allosteric modulation and positive allosteric modulation.[27] Interestingly, here we also observed inverse agonism, although with very low efficacy: only 14% at highest (**23** in CCR8).

For the meta position, the double methylation in **2** and **6** (**Bip** and **Phe** analogs, respectively) is more favored in CCR5, which is also the only receptor activated by the meta-thiomethylated **23.** This suggests that such "wide" compounds are positioned in a way that they block helices from closing in to each other in CCR1 and CCR8, but not in CCR5. Different binding modes could also be the explanation for the

dx.doi.org/10.1021/ci4003848 | J. Chem. Inf. Model. XXXX, XXX, XXX−XXX

inconsistent assaying results for the 5-substituted **Phe** analogs. Specifically, for CCR1 and CCR8 the potencies are surprisingly similar for the different methyl (**11**), chloro (**12**), and amino (**26**) substituents. The chelators are very flexible around the site of chelation and the proximal receptor cavities can be polar on one side and hydrophobic on the other. The potencies of 5-methylated compounds in CCR5 are even more peculiar as the two published chelators, **11** and **12**, were both inactive whereas the two new, **26** and **27**, are active. This could partly be due to the fact that the latter have more electron-donating substituents, but still it is difficult to envision why the extra 6-methyl in **27** compared to single 5-methylation in **11** leads from inactivity to 2 μM potency. The flexibility of the chelators within the binding site and existence of only one specific interaction will likely make receptor structure-based ligand design more challenging.

CONCLUSIONS

We have described in-depth SAR for the activity of three metal-ion chelator scaffold series; 2,2′-bipyridine, 1,10-phenanthroline, and 2,2′;6′,2″-terpyridine at the CCR1, CCR8, and CCR5 chemokine receptors. Density functional theory calculations showed that the electron donating and withdrawing effects of substituents directly influence the partial charges of chelating nitrogen atoms and zinc affinities. The zinc affinity was found to constitute the major factor for receptor potency. Most inactive chelators display steric hindrance from ortho-substituents or a tautomer state with protonated chelating nitrogens. Hydrophobic and halogen substituents are generally better accommodated by the receptors than polar. For each receptor, the structure−activity relationships for potency and selectivity were determined, leading to the selection of a new series comprising eight chelators. Pharmacological testing resulted in chelators with higher potency in CCR1 **28** and **29** and CCR8 **29**. Furthermore, we identified the first fully selective CCR5 chelator, **23** (previously the best CCR5-selectivity was 3.2-fold). We also showed a new type of action, inverse agonism, although very weak (at highest 14% by **23** in CCR8).

EXPERIMENTAL SECTION

Quantum Mechanics Calculations of Partial Charges and Bip Pyridine Rotation Energies. Density functional theory calculations were performed with the Turbomole software package version 6.3.1,[30] using the TPSS functional[42] with D3 dispersion correction,[43] the def-SV(P) basis set,[44,45] and the resolution of identity approximation.[44,46,4748,50,51] Solvation effects were computed using the continuum conductor-like screening model (COSMO)[48] using an effective dielectric constant (ε) of 80. All geometries were verified to be minima by frequency calculations. A subset of chelators had to be excluded from this analysis due to no (**1**) or untested (**14**) zinc affinity. Furthermore, the ortho-substituted chelators could only be included if correlated separately (Figure 1c).

Calculation of LogP, Charge, and Tautomer States. LogP values were calculated with QikProp version 3.5. The ionization and tautomer states of all chelators were calculated with Schrödinger LigPrep[49] and Epik[32,50] using the OPLS-2005 force field. The pH was set to 7.2 ± 0.2 (that of the Hanks' solution used in the assays), and the calculation was set to include metal binding states. The partial charges of **13.1**−**3** were calculated with Turbomole as described above.

Analysis of Zinc Affinity and Receptor Potency Data. Graphs of zinc affinity and receptor potency data were produced in Microsoft Excel 2010 and edited in Inkscape. Chelator structures were drawn in ChemBioDraw Ultra 12. The merged-structures for Chart 2 were drawn in ChemBioDraw Ultra 12, exported to a single mol2 file, and imported in Pymol.[51] The Pymol aromaticity-estimate was unsuccessful for the **Phe**-scaffold; therefore, the resulting image was retouched in GIMP to remove the excess double bonds.

Selection of New Chelator Analogs. We performed a substructure search in eMolecules (www.eMolecules.com) for new chelator analogs using **Bip** as the query. Chelators were purchased from Sigma Aldrich **23** (5,5′-bis(mercaptomethyl)-2,2′-bipyridine), **25** ((2-(4′-(2-dimethylamino-vinyl)-(2,2′)-bipyridinyl-4-yl)-vinyl)-dimethyl-amine), and **26** (1,10-phenanthrolin-5-amine); TCI Europe **22** (4,4′-bis(hydroxymethyl)-2,2′-bipyridine), **24** (4,4′-bis(chloromethyl)-2,2′-bipyridyl), **27** (5,6-dimethyl-1,10-phenanthroline), and **29** (4′-bromo-2,2′:6′,2″-terpyridine), and Florida Center for Heterocyclic Compounds: **28** (4,7-dipropyl-phenanthrolin).

Experimental Materials. The human chemokines CCL1, CCL3, and CCL5 were purchased from Peprotech (NJ, USA). The highest concentration of metal ion chelator complexes ZnBip and ZnPhe were made from 0.2 M $ZnCl_2$ in water, 0.2 M $CuSO_4$ in water, 0.4 M phenanthroline in 70% ethanol, and 0.4 M bipyridine in DMSO and were supplemented with 10% DMSO, water, and 70% ethanol. Chelator analogs were dissolved in DMSO to 10 mM, except for 22 and 26 that were dissolved in water and prepared in similar ways. Dilutions were made in water. Receptor CCR5 was cloned in house from a leukocyte cDNA library, CCR1 cDNA was kindly provided by Tim Wells (GlaxoSmithKline, UK), and CCR8 was purchased from cDNA.org. The promiscuous G protein $G\alpha_{\Delta 6qi4myr}$ was kindly provided by Evi Kostenis (University of Bonn, Germany). Myo-[3*H*]inositol (PT6-271) was purchased from PerkinElmer (MA, USA). AG 1-X8 anion exchange resin was from Bio-Rad (CA, USA).

Zn(II)-Affinity Assaying. A 10 μL portion of the chelator was added to 90 μL of reaction buffer containing 20 nM ZnCl, 1 μM FluoZin-3 (Invitrogen, UK), 10 mM LiCl in Hanks balanced salt solution (Invitrogen, UK). After 2 h incubation at room temperature, fluorescence intensity (excitation at 485 nm and emission at 520 nm) was measured in a POLARstar Omega from BMG Labtech.

Receptor Assaying. *Transfections and Tissue Culture.* COS-7 cells were grown at 10% CO_2 and 37 °C in Dulbecco's modified Eagle's medium with glutamax (Invitrogen, UK) adjusted with 10% fetal bovine serum, 180 units/mL penicillin, and 45 μg/mL penicillin/streptomycin (PenStrep). Transfection of the COS-7 cells was performed by the calcium phosphate precipitation method.[52]

Inositol Phosphate Turnover (IP Turnover). COS-7 cells were transfected according to the procedure mentioned above. Briefly, 6×10^6 cells were transfected with 20 μg of receptor cDNA in addition to 30 μg of the promiscuous chimeric G protein, $G\alpha_{qi4myr}$, which turns the $G\alpha_i$-coupled signal, the most common pathway for endogenous chemokine receptors, into the $G\alpha_q$ pathway (phospholipase C activation measured as IP_3 turnover).[52,53] From here, two different assays differing in their scale, but which were found to show the same result, were carried out. A "traditional" IP_3-assay was carried out as described previously.[27] The new compounds were solely tested with the Scintillation proximity assay (SPA)—IP_3: One day

dx.doi.org/10.1021/ci4003848 | J. Chem. Inf. Model. XXXX, XXX, XXX−XXX

after transfection, COS-7 cells (35.000 cells/well) were incubated for 24 h with 0.5 μCi/mL *myo*[^{3}H]inositol in 100 μL of growth medium per well in a 96-well plate. Cells were washed twice in PBS and were incubated in 0.1 mL Hank's Balanced Salt Solution (Invitrogen, UK) supplemented with 10 mM LiCl at 37 °C in the presence of various concentrations of ligands. Cells were extracted by addition of 50 μL of 10 mM formic acid to each well followed by incubation on ice for 30−60 min. A 20 μL of the extract was transferred to a white 96-well plate and 80 μL of 1:8 diluted YSi poly-D-lysine coated beads (Perkin-Elmer, MA, USA) were added. Plates were sealed and shaken at maximum speed for at least 30 min and centrifuged for 5 min at 1500 rpm, and γ-radiation was counted in a Packard Top Count NXT counter. In both assays, determinations were made in duplicates. This general read-out has previously been used with success in other chemokine receptors.[25,54]

■ ASSOCIATED CONTENT

Supporting Information

Table SI1: Partial charges, zinc affinities, potencies and efficacies of published chelators. Figure SI2: Size comparison for **Phe** ortho-analogs. Figure SI3: Chelator selectivities. Chart SI3: Protonation and tautomer states of **13**. This material is available free of charge via the Internet at http://pubs.acs.org.

■ AUTHOR INFORMATION

Corresponding Author

*Phone: (+45) 353 36162. Fax: (+45) 35 33 60 41. E-mail: david.gloriam@sund.ku.dk.

Notes

The authors declare no competing financial interest.

■ ACKNOWLEDGMENTS

D.E.G. and V.I. were supported by the Carlsberg and Lundbeck Foundations, respectively. P.R. received financial support from Lhasa Limited. M.M.R. and S.T. were supported by the Danish Council for Independent Research/Medical Sciences, the NovoNordisk Foundation, the Lundbeck Foundation, the European Community's Sixth Framework program (INNO-CHEM: Grant LSHB-CT-2005-518167), the AP-Moller Foundation, and the Aase and Einar Danielsen Foundation. We thank Randi Thøgersen and Inger Smith Simonsen for excellent technical assistance.

■ ABBREVIATIONS

7TM, Seven transmembrane receptor; CCR1, CC chemokine receptor1; CCR5, CC chemokine receptor5; CCR8, CC chemokine receptor8; CCL3, CC chemokine ligand3; CCL5, CC chemokine ligand5; GPCR, G protein-coupled receptor

■ REFERENCES

(1) Venter, J. C.; Adams, M. D.; Myers, E. W.; Li, P. W.; Mural, R. J.; Sutton, G. G.; Smith, H. O.; Yandell, M.; Evans, C. A.; Holt, R. A.; Gocayne, J. D.; Amanatides, P.; Ballew, R. M.; Huson, D. H.; Wortman, J. R.; Zhang, Q.; Kodira, C. D.; Zheng, X. H.; Chen, L.; Skupski, M.; Subramanian, G.; Thomas, P. D.; Zhang, J.; Gabor Miklos, G. L.; Nelson, C.; Broder, S.; Clark, A. G.; Nadeau, J.; McKusick, V. A.; Zinder, N.; Levine, A. J.; Roberts, R. J.; Simon, M.; Slayman, C.; Hunkapiller, M.; Bolanos, R.; Delcher, A.; Dew, I.; Fasulo, D.; Flanigan, M.; Florea, L.; Halpern, A.; Hannenhalli, S.; Kravitz, S.; Levy, S.; Mobarry, C.; Reinert, K.; Remington, K.; Abu-Threideh, J.; Beasley, E.; Biddick, K.; Bonazzi, V.; Brandon, R.; Cargill, M.; Chandramouliswaran, I.; Charlab, R.; Chaturvedi, K.; Deng, Z.; Di Francesco, V.; Dunn, P.; Eilbeck, K.; Evangelista, C.; Gabrielian, A. E.; Gan, W.; Ge, W.; Gong, F.; Gu, Z.; Guan, P.; Heiman, T. J.; Higgins, M. E.; Ji, R. R.; Ke, Z.; Ketchum, K. A.; Lai, Z.; Lei, Y.; Li, Z.; Li, J.; Liang, Y.; Lin, X.; Lu, F.; Merkulov, G. V.; Milshina, N.; Moore, H. M.; Naik, A. K.; Narayan, V. A.; Neelam, B.; Nusskern, D.; Rusch, D. B.; Salzberg, S.; Shao, W.; Shue, B.; Sun, J.; Wang, Z.; Wang, A.; Wang, X.; Wang, J.; Wei, M.; Wides, R.; Xiao, C.; Yan, C.; Yao, A.; Ye, J.; Zhan, M.; Zhang, W.; Zhang, H.; Zhao, Q.; Zheng, L.; Zhong, F.; Zhong, W.; Zhu, S.; Zhao, S.; Gilbert, D.; Baumhueter, S.; Spier, G.; Carter, C.; Cravchik, A.; Woodage, T.; Ali, F.; An, H.; Awe, A.; Baldwin, D.; Baden, H.; Barnstead, M.; Barrow, I.; Beeson, K.; Busam, D.; Carver, A.; Center, A.; Cheng, M. L.; Curry, L.; Danaher, S.; Davenport, L.; Desilets, R.; Dietz, S.; Dodson, K.; Doup, L.; Ferriera, S.; Garg, N.; Gluecksmann, A.; Hart, B.; Haynes, J.; Haynes, C.; Heiner, C.; Hladun, S.; Hostin, D.; Houck, J.; Howland, T.; Ibegwam, C.; Johnson, J.; Kalush, F.; Kline, L.; Koduru, S.; Love, A.; Mann, F.; May, D.; McCawley, S.; McIntosh, T.; McMullen, I.; Moy, M.; Moy, L.; Murphy, B.; Nelson, K.; Pfannkoch, C.; Pratts, E.; Puri, V.; Qureshi, H.; Reardon, M.; Rodriguez, R.; Rogers, Y. H.; Romblad, D.; Ruhfel, B.; Scott, R.; Sitter, C.; Smallwood, M.; Stewart, E.; Strong, R.; Suh, E.; Thomas, R.; Tint, N. N.; Tse, S.; Vech, C.; Wang, G.; Wetter, J.; Williams, S.; Williams, M.; Windsor, S.; Winn-Deen, E.; Wolfe, K.; Zaveri, J.; Zaveri, K.; Abril, J. F.; Guigo, R.; Campbell, M. J.; Sjolander, K. V.; Karlak, B.; Kejariwal, A.; Mi, H.; Lazareva, B.; Hatton, T.; Narechania, A.; Diemer, K.; Muruganujan, A.; Guo, N.; Sato, S.; Bafna, V.; Istrail, S.; Lippert, R.; Schwartz, R.; Walenz, B.; Yooseph, S.; Allen, D.; Basu, A.; Baxendale, J.; Blick, L.; Caminha, M.; Carnes-Stine, J.; Caulk, P.; Chiang, Y. H.; Coyne, M.; Dahlke, C.; Mays, A.; Dombroski, M.; Donnelly, M.; Ely, D.; Esparham, S.; Fosler, C.; Gire, H.; Glanowski, S.; Glasser, K.; Glodek, A.; Gorokhov, M.; Graham, K.; Gropman, B.; Harris, M.; Heil, J.; Henderson, S.; Hoover, J.; Jennings, D.; Jordan, C.; Jordan, J.; Kasha, J.; Kagan, L.; Kraft, C.; Levitsky, A.; Lewis, M.; Liu, X.; Lopez, J.; Ma, D.; Majoros, W.; McDaniel, J.; Murphy, S.; Newman, M.; Nguyen, T.; Nguyen, N.; Nodell, M.; Pan, S.; Peck, J.; Peterson, M.; Rowe, W.; Sanders, R.; Scott, J.; Simpson, M.; Smith, T.; Sprague, A.; Stockwell, T.; Turner, R.; Venter, E.; Wang, M.; Wen, M.; Wu, D.; Wu, M.; Xia, A.; Zandieh, A.; Zhu, X. The sequence of the human genome. *Science* **2001**, *291*, 1304−1351.

(2) Overington, J. P.; Al-Lazikani, B.; Hopkins, A. L. How many drug targets are there? *Nat. Rev. Drug Discov.* **2006**, *5*, 993−996.

(3) Rosenkilde, M. M.; Schwartz, T. W. The chemokine system – a major regulator of angiogenesis in health and disease. *APMIS* **2004**, *112*, 481−495.

(4) Viola, A.; Luster, A. D. Chemokines and their receptors: drug targets in immunity and inflammation. *Annu. Rev. Pharmacol. Toxicol.* **2008**, *48*, 171−197.

(5) Scholten, D. J.; Canals, M.; Maussang, D.; Roumen, L.; Smit, M. J.; Wijtmans, M.; de Graaf, C.; Vischer, H. F.; Leurs, R. Pharmacological modulation of chemokine receptor function. *Br. J. Pharmacol.* **2012**, *165*, 1617−1643.

(6) Horuk, R. Promiscuous drugs as therapeutics for chemokine receptors. *Exp. Rev. Mol. Med.* **2009**, *11*, e1.

(7) Pease, J. E.; Horuk, R. Small molecule antagonists of chemokine receptors–is promiscuity a virtue? *Curr. Top. Med. Chem.* **2010**, *10*, 1351−1358.

(8) Allen, S. J.; Crown, S. E.; Handel, T. M. Chemokine: receptor structure, interactions, and antagonism. *Annu. Rev. Immunol.* **2007**, *25*, 787−820.

(9) Murphy, P. M. International Union of Pharmacology. XXX. Update on chemokine receptor nomenclature. *Pharmacol. Rev.* **2002**, *54*, 227−229.

(10) Rosenkilde, M. M.; Schwartz, T. W. GluVII:06–a highly conserved and selective anchor point for non-peptide ligands in chemokine receptors. *Curr. Top. Med. Chem.* **2006**, *6*, 1319−1333.

(11) Oteiza, P. I.; Mackenzie, G. G. Zinc, oxidant-triggered cell signaling, and human health. *Mol. Aspects Med.* **2005**, *26*, 245−255.

(12) Norregaard, L.; Frederiksen, D.; Nielsen, E. O.; Gether, U. Delineation of an endogenous zinc-binding site in the human dopamine transporter. *EMBO J.* **1998**, *17*, 4266−4273.
(13) Hsiao, B.; Dweck, D.; Luetje, C. W. Subunit-dependent modulation of neuronal nicotinic receptors by zinc. *J. Neurosci.* **2001**, *21*, 1848−1856.
(14) Rosenkilde, M. M.; Lucibello, M.; Holst, B.; Schwartz, T. W. Natural agonist enhancing bis-His zinc-site in transmembrane segment V of the tachykinin NK3 receptor. *FEBS Lett.* **1998**, *439*, 35−40.
(15) Storjohann, L.; Holst, B.; Schwartz, T. W. Molecular mechanism of Zn2+ agonism in the extracellular domain of GPR39. *FEBS Lett.* **2008**, *582*, 2583−2588.
(16) Takeda, A.; Minami, A.; Seki, Y.; Oku, N. Differential effects of zinc on glutamatergic and GABAergic neurotransmitter systems in the hippocampus. *J. Neurosci. Res.* **2004**, *75*, 225−229.
(17) Elling, C. E.; Thirstrup, K.; Holst, B.; Schwartz, T. W. Conversion of agonist site to metal-ion chelator site in the beta(2)-adrenergic receptor. *Proc. Natl. Acad. Sci. U. S. A.* **1999**, *96*, 12322−12327.
(18) Rosenkilde, M. M.; Andersen, M. B.; Nygaard, R.; Frimurer, T. M.; Schwartz, T. W. Activation of the CXCR3 chemokine receptor through anchoring of a small molecule chelator ligand between TM-III, -IV, and -VI. *Mol. Pharmacol.* **2007**, *71*, 930−941.
(19) Holst, B.; Elling, C. E.; Schwartz, T. W. Partial Agonism through a Zinc-Ion Switch Constructed between Transmembrane Domains III and VII in the Tachykinin NK1 Receptor. *Mol. Pharmacol.* **2000**, *58*, 263−270.
(20) Schwartz, T. W.; Frimurer, T. M.; Holst, B.; Rosenkilde, M. M.; Elling, C. E. Molecular mechanism of 7TM receptor activation–a global toggle switch model. *Annu. Rev. Pharmacol. Toxicol.* **2006**, *46*, 481−519.
(21) Elling, C. E.; Frimurer, T. M.; Gerlach, L. O.; Jorgensen, R.; Holst, B.; Schwartz, T. W. Metal ion site engineering indicates a global toggle switch model for seven-transmembrane receptor activation. *J. Biol. Chem.* **2006**, *281*, 17337−17346.
(22) Xu, F.; Wu, H.; Katritch, V.; Han, G. W.; Jacobson, K. A.; Gao, Z. G.; Cherezov, V.; Stevens, R. C. Structure of an agonist-bound human A2A adenosine receptor. *Science* **2011**, *332*, 322−327.
(23) Warne, T.; Moukhametzianov, R.; Baker, J. G.; Nehme, R.; Edwards, P. C.; Leslie, A. G.; Schertler, G. F.; Tate, C. G. The structural basis for agonist and partial agonist action on a beta(1)-adrenergic receptor. *Nature* **2011**, *469*, 241−244.
(24) Rasmussen, S. G.; DeVree, B. T.; Zou, Y.; Kruse, A. C.; Chung, K. Y.; Kobilka, T. S.; Thian, F. S.; Chae, P. S.; Pardon, E.; Calinski, D.; Mathiesen, J. M.; Shah, S. T.; Lyons, J. A.; Caffrey, M.; Gellman, S. H.; Steyaert, J.; Skiniotis, G.; Weis, W. I.; Sunahara, R. K.; Kobilka, B. K. Crystal structure of the beta2 adrenergic receptor-Gs protein complex. *Nature* **2011**, *477*, 549−555.
(25) Jensen, P. C.; Thiele, S.; Ulven, T.; Schwartz, T. W.; Rosenkilde, M. M. Positive versus negative modulation of different endogenous chemokines for CC-chemokine receptor 1 by small molecule agonists through allosteric versus orthosteric binding. *J. Biol. Chem.* **2008**, *283*, 23121−23128.
(26) Thiele, S.; Steen, A.; Jensen, P. C.; Mokrosinski, J.; Frimurer, T. M.; Rosenkilde, M. M. Allosteric and orthosteric sites in CC chemokine receptor (CCR5), a chimeric receptor approach. *J. Biol. Chem.* **2011**, *286*, 37543−37554.
(27) Thiele, S.; Malmgaard-Clausen, M.; Engel-Andreasen, J.; Steen, A.; Rummel, P. C.; Nielsen, M. C.; Gloriam, D. E.; Frimurer, T. M.; Ulven, T.; Rosenkilde, M. M. Modulation in selectivity and allosteric properties of small-molecule ligands for CC-chemokine receptors. *J. Med. Chem.* **2012**, *18*, 8164−8177.
(28) Rosenkilde, M. M.; Kledal, T. N.; Brauner-Osborne, H.; Schwartz, T. W. Agonists and Inverse Agonists for the Herpesvirus 8-encoded Constitutively Active Seven-transmembrane Oncogene Product, ORF-74. *J. Biol. Chem.* **1999**, *274*, 956−961.
(29) Rosenkilde, M. M.; David, R.; Oerlecke, I.; Benned-Jensen, T.; Geumann, U.; Beck-Sickinger, A. G.; Schwartz, T. W. Conformational constraining of inactive and active States of a seven transmembrane receptor by metal ion site engineering in the extracellular end of transmembrane segment V. *Mol. Pharmacol.* **2006**, *70*, 1892−1901.
(30) Ahlrichs, R.; Bär, M.; Häser, M.; Horn, H.; Kölmel, C. Electronic structure calculations on workstation computers: The program system turbomole. *Chem. Phys. Lett.* **1989**, *162*, 165−169.
(31) Bortolato, A.; Tehan, B. G.; Bodnarchuk, M. S.; Essex, J. W.; Mason, J. S. Water network perturbation in ligand binding: adenosine A(2A) antagonists as a case study. *J. Chem Inf. Model.* **2013**, *53*, 1700−1713.
(32) Shelley, J. C.; Cholleti, A.; Frye, L. L.; Greenwood, J. R.; Timlin, M. R.; Uchimaya, M. Epik: a software program for pK(a) prediction and protonation state generation for drug-like molecules. *J. Comput. Aided Mol. Des.* **2007**, *21*, 681−691.
(33) Wijtmans, M.; Scholten, D. J.; Roumen, L.; Canals, M.; Custers, H.; Glas, M.; Vreeker, M. C.; de Kanter, F. J.; de Graaf, C.; Smit, M. J.; de Esch, I. J.; Leurs, R. Chemical subtleties in small-molecule modulation of peptide receptor function: the case of CXCR3 biaryl-type ligands. *J. Med. Chem.* **2012**, *55*, 10572−10583.
(34) Holst, B.; Mokrosinski, J.; Lang, M.; Brandt, E.; Nygaard, R.; Frimurer, T. M.; Beck-Sickinger, A. G.; Schwartz, T. W. Identification of an efficacy switch region in the ghrelin receptor responsible for interchange between agonism and inverse agonism. *J. Biol. Chem.* **2007**, *282*, 15799−15811.
(35) Baba, M.; Nishimura, O.; Kanzaki, N.; Okamoto, M.; Sawada, H.; Iizawa, Y.; Shiraishi, M.; Aramaki, Y.; Okonogi, K.; Ogawa, Y.; Meguro, K.; Fujino, M. A small-molecule, nonpeptide CCR5 antagonist with highly potent and selective anti-HIV-1 activity. *Proc. Natl. Acad. Sci. U. S. A.* **1999**, *96*, 5698−5703.
(36) Seto, M.; Aikawa, K.; Miyamoto, N.; Aramaki, Y.; Kanzaki, N.; Takashima, K.; Kuze, Y.; Iizawa, Y.; Baba, M.; Shiraishi, M. Highly potent and orally active CCR5 antagonists as anti-HIV-1 agents: synthesis and biological activities of 1-benzazocine derivatives containing a sulfoxide moiety. *J. Med. Chem.* **2006**, *49*, 2037−2048.
(37) Sabroe, I.; Peck, M. J.; Van Keulen, B. J.; Jorritsma, A.; Simmons, G.; Clapham, P. R.; Williams, T. J.; Pease, J. E. A small molecule antagonist of chemokine receptors CCR1 and CCR3. Potent inhibition of eosinophil function and CCR3-mediated HIV-1 entry. *J. Biol. Chem.* **2000**, *275*, 25985−25992.
(38) Allegretti, M.; Bertini, R.; Cesta, M. C.; Bizzarri, C.; Di Bitondo, R.; Di Cioccio, V.; Galliera, E.; Berdini, V.; Topai, A.; Zampella, G.; Russo, V.; Di Bello, N.; Nano, G.; Nicolini, L.; Locati, M.; Fantucci, P.; Florio, S.; Colotta, F. 2-Arylpropionic CXC chemokine receptor 1 (CXCR1) ligands as novel noncompetitive CXCL8 inhibitors. *J. Med. Chem.* **2005**, *48*, 4312−4331.
(39) Dwyer, M. P.; Yu, Y.; Chao, J.; Aki, C.; Biju, P.; Girijavallabhan, V.; Rindgen, D.; Bond, R.; Mayer-Ezel, R.; Jakway, J.; Hipkin, R. W.; Fossetta, J.; Gonsiorek, W.; Bian, H.; Fan, X.; Terminelli, C.; Fine, J.; Lundell, D.; Merritt, J. R.; Rokosz, L. L.; Kaiser, B.; Li, G.; Wang, W.; Stauffer, T.; Ozgur, L.; Baldwin, J.; Taveras, A. G. Discovery of 2-hydroxy-N,N-dimethyl-3-{2-[[(R)-1-(5- methylfuran-2-yl)propyl]-amino]-3,4-dioxocyclobut-1-enylamino}benzamide (SCH 527123): a potent, orally bioavailable CXCR2/CXCR1 receptor antagonist. *J. Med. Chem.* **2006**, *49*, 7603−7606.
(40) Princen, K.; Hatse, S.; Vermeire, K.; Aquaro, S.; De Clercq, E.; Gerlach, L. O.; Rosenkilde, M.; Schwartz, T. W.; Skerlj, R.; Bridger, G.; Schols, D. Inhibition of human immunodeficiency virus replication by a dual CCR5/CXCR4 antagonist. *J. Virol.* **2004**, *78*, 12996−13006.
(41) Walters, I.; Austin, C.; Austin, R.; Bonnert, R.; Cage, P.; Christie, M.; Ebden, M.; Gardiner, S.; Grahames, C.; Hill, S.; Hunt, F.; Jewell, R.; Lewis, S.; Martin, I.; David, N.; David, R. Evaluation of a series of bicyclic CXCR2 antagonists. *Bioorg. Med. Chem. Lett.* **2008**, *18*, 798−803.
(42) Tao, J.; Perdew, J. P.; Staroverov, V. N.; Scuseria, G. E. Climbing the density functional ladder: nonempirical meta-generalized gradient approximation designed for molecules and solids. *Phys. Rev. Lett.* **2003**, *91*, 146401.
(43) Grimme, S.; Antony, J.; Ehrlich, S.; Krieg, H. A consistent and accurate ab initio parametrization of density functional dispersion

correction (DFT-D) for the 94 elements H-Pu. *J. Chem. Phys.* **2010**, *132*, 154104.
(44) Eichkorn, K.; Treutler, O.; Öhm, H.; Häser, M.; Ahlrichs, R. Auxiliary basis sets to approximate Coulomb potentials (Chem. Phys. Letters 240 (1995) 283−290). *Chem. Phys. Lett.* **1995**, *242*, 652−660.
(45) Schafer, A.; Horn, H.; Ahlrichs, R. Fully optimized contracted Gaussian basis sets for atoms Li to Kr. *J. Chem. Phys.* **1992**, *97*, 2571−2577.
(46) Eichkorn, K.; Weigend, F.; Treutler, O.; Ahlrichs, R. Auxiliary basis sets for main row atoms and transition metals and their use to approximate Coulomb potentials. *Theor. Chem. Accounts: Theory, Comput. Model.* **1997**, *97*, 119−124.
(47) Weigend, F. Accurate Coulomb-fitting basis sets for H to Rn. *Phys. Chem. Chem. Phys.* **2006**, *8*, 1057−1065.
(48) Klamt, A.; Schuurmann, G. COSMO: a new approach to dielectric screening in solvents with explicit expressions for the screening energy and its gradient. *J. Chem. Soc., Perkin Trans. 2* **1993**, 799−805.
(49) *LigPrep*, 2.5; Schrödinger LLC: New York, 2011.
(50) Greenwood, J. R.; Calkins, D.; Sullivan, A. P.; Shelley, J. C. Towards the comprehensive, rapid, and accurate prediction of the favorable tautomeric states of drug-like molecules in aqueous solution. *J. Comput. Aided Mol. Des.* **2010**, *24*, 591−604.
(51) *The PyMOL Molecular Graphics System*, 1.5.0.4; Schrödinger LCC: New York, 2012.
(52) Rosenkilde, M. M.; Cahir, M.; Gether, U.; Hjorth, S. A.; Schwartz, T. W. Mutations along transmembrane segment II of the NK-1 receptor affect substance P competition with non-peptide antagonists but not substance P binding. *J. Biol. Chem.* **1994**, *269*, 28160−28164.
(53) Kostenis, E.; Zeng, F. Y.; Wess, J. Functional characterization of a series of mutant G protein alphaq subunits displaying promiscuous receptor coupling properties. *J. Biol. Chem.* **1998**, *273*, 17886−17892.
(54) Jensen, P. C.; Nygaard, R.; Thiele, S.; Elder, A.; Zhu, G.; Kolbeck, R.; Ghosh, S.; Schwartz, T. W.; Rosenkilde, M. M. Molecular interaction of a potent nonpeptide agonist with the chemokine receptor CCR8. *Mol. Pharmacol.* **2007**, *72*, 327−340.